The impact of a Southern Ocean cyclonic eddy on mesopelagic micronekton

Alice Della Penna[1], Joan Llort[2], Sebastien Moreau[3], Ramkrushnbhai S Patel[3], Rudy J. Kloser[4], Peter Gaube[5], Peter G. Strutton[6], and Philip W Boyd[3]

[1]University of Auckland
[2]Barcelona Supercomputing Center
[3]Institute for Marine and Antarctic Studies
[4]CSIRO Oceans and Atmosphere
[5]Applied Physics Laboratory
[6]University of Tasmania

November 23, 2022

Abstract

Southern Ocean eddies shape the foraging ecology of marine apex predators such as marine mammals and seabirds. A growing number of animal tracking studies show that predators alter their swimming, diving, and foraging behavior in mesoscale eddies. However, little is known about how Southern Ocean eddies influence the distribution of mesopelagic micronekton (fish, squid, and crustaceans), which are major prey items of megafauna. Studies in other parts of the world have found that eddies can impact the abundance and community composition of micronekton. Here, we analyze acoustic observations from a 14-day survey of a mesoscale eddy, its surrounding waters, and the Sub-Antarctic frontal waters where the eddy originated. We report and interpret spatial patterns of acoustic backscattering at 18 kHz, a proxy indicating combined changes in species, size, and abundance of micronekton. We find that the vertical distribution of Deep Scattering Layers matched the underwater light conditions characteristic of the eddy core, periphery, and surrounding waters, at scales smaller than 10 km. Furthermore, the average water-column integrated acoustic backscattering values in the eddy core were only half of the values measured in the Sub-Antarctic Zone waters surrounding the eddy. By contrast, the acoustic properties of the eddy core were similar to those measured in the Polar Front Zone, where the eddy originated 27 days before our sampling. These results show that, as for physical and chemical tracers, the eddy maintained its biological characteristics from its source waters creating a unique habitat compared to its surrounding waters.

The impact of a Southern Ocean cyclonic eddy on mesopelagic micronekton

Alice Della Penna[1,2], Joan Llort[3], Sebastien Moreau[4], Ramkrushnbhai Patel[5,6], Rudy Kloser[7], Peter Gaube[8], Peter Strutton[5], Philip Boyd[5];

1. Institute of Marine Science, University of Auckland, New Zealand
2. School of Biological Sciences, University of Auckland, New Zealand
3. Barcelona Supercomputing Center, Barcelona, Spain
4. Norwegian Polar Institute, Fram Center, Tromsø, Norway
5. Institute for Marine and Antarctic Studies (IMAS), University of Tasmania (UTas), Hobart, Tasmania, Australia
6. Australian Research Council Centre of Excellence for Climate System Science, University of Tasmania, Hobart, Tasmania, Australia
7. CSIRO Oceans and Atmosphere, GPO Box 1538, Hobart, Tasmania, 7001, Australia
8. Applied Physics Laboratory, University of Washington, Seattle, Washington, United States of America

Corresponding author: Alice Della Penna (alice.dellapenna@gmail.com)

Key Points:

- We observed the distribution of Deep Scattering Layers (DSL) in the mesopelagic across a Southern Ocean cyclonic eddy.
- Acoustic properties such as integrated backscattering and DSL distribution within the cyclonic eddy were similar to its origin waters.
- The eddy presented a unique habitat compared to its surrounding waters, affecting the accessibility of mesopelagic prey to diving predators.

Abstract

Southern Ocean eddies shape the foraging ecology of marine apex predators such as marine mammals and seabirds. A growing number of animal tracking studies show that predators alter their swimming, diving, and foraging behavior in mesoscale eddies. However, little is known about how Southern Ocean eddies influence the distribution of mesopelagic micronekton (fish, squid, and crustaceans), which are major prey items of megafauna. Studies in other parts of the world have found that eddies can impact the abundance and community composition of micronekton. Here, we analyze acoustic observations from a 14-day survey of a mesoscale eddy, its surrounding waters, and the Sub-Antarctic frontal waters where the eddy originated. We report and interpret spatial patterns of acoustic backscattering at 18 kHz, a proxy indicating combined changes in species, size, and abundance of micronekton. We find that the vertical distribution of Deep Scattering Layers matched the underwater light conditions characteristic of the eddy core, periphery, and surrounding waters, at scales smaller than 10 km. Furthermore, the average water-column integrated acoustic backscattering values in the eddy core were only half of the values measured in the Sub-Antarctic Zone waters surrounding the eddy. By contrast, the acoustic properties of the eddy core were similar to those measured in the Polar Front Zone, where the eddy originated 27 days before our sampling. These results show that, as for physical

and chemical tracers, the eddy maintained its biological characteristics from its source waters creating a unique habitat compared to its surrounding waters.

Plain language summary

Mesoscale eddies are rotating currents that are ubiquitous in the ocean. They are the oceanic equivalent of weather patterns and have typically radii of 10-100 km and lifetimes between weeks and months. Mesoscale eddies have a dramatic impact on the distribution of primary production in the open ocean, on the transport of heat and salt across oceanic regions, on global biogeochemical cycles, and on the feeding behavior of apex predators such as pinnipeds, sharks, billfishes, and seabirds. In this study, we evaluated the impact of a Southern Ocean mesoscale eddy on the distribution of deep water micronekton, a diverse group of small animals including fish, crustacea, and squids. We found that the abundance and vertical distribution of deep water micronekton, detected using a sonar, inside the sampled mesoscale eddy differed from those of the surrounding waters. Micronekton distribution and abundance were instead more similar to those of the locations where the eddy had originated a month prior to our sampling. Our results suggest that mesoscale eddies can maintain their biological characteristics from its source waters creating a unique habitat compared to its surrounding waters.

1 Introduction

Southern Ocean mesoscale eddies, rotating currents characterized by spatio-temporal scales of 10-100 km and lifetimes weeks-months, are key foraging regions for top marine predators such as mammals (Campagna et al., 2006; Dragon et al., 2010; Bailleul et al. 2010; Della Penna et al., 2015; Cotté et al., 2015) and seabirds (Cotté et al., 2007). These animals forage primarily on micronekton, including small fish, cephalopods and crustaceans, and mesozooplankton, which mostly inhabit the mesopelagic zone (the stratum lying between 200 and 1000 m depth; McMahon et al., 2019).

Despite their importance for marine ecosystems (Murphy et al., 2016; Subramanian et al., 2020), little is known about mesopelagic micronekton and how mesoscale eddies may affect their distribution. These organisms are challenging to observe: they are too small to be tagged with the animal tracking devices used to study top predators and are invisible to our current satellite sensors, which are generally limited to observing the near-surface of the ocean. Current methods to observe mesopelagic micronekton include mid-water trawling (Wiebe et al.,1985; Greene et al. 1990), optical devices (Kloser et al., 2016) and acoustic methods (Kloser et al., 2009; Ryan et al., 2009). Furthermore, micronekton varies at many temporal and spatial scales. These include the scales spanning diel vertical migration behavior (DVM; Cuvier, 1817; Hays, 2003) to seasonal and inter-annual variability (Urmy et al.,2016; Escobar-Flores et al., 2018). Disentangling this variability in the remote Southern Ocean is further complicated by the logistical challenges of collecting ship-based data in the often harsh conditions of this region.

In recent years, the number of observations of acoustic backscattering has been growing, resulting in the creation of datasets of multi-frequency observations from research vessels and ships of opportunity (Kunnath et al., 2021). These new observations facilitate an analysis of the

spatial distribution of biogeographical provinces, or bio-regions, for mesopelagic organisms (*e.g.*, Proud et al. 2015; Klevjer et al. 2016). Bio-regions define the large-scale habitat of the marine animals that prey on mesopelagic nekton. Yet, such bio-regions do not capture the fine-scale variability that highly mobile predators encounter during their foraging trips. This variability is largely influenced by mesoscale and submesoscale features such as fronts, filaments, and eddies (Tew-Kai et al., 2009; Bost et al., 2009; Gaube et al., 2018; Braun et al., 2019; Chapman et al., 2020) and is central in understanding the role of patchiness in modulating biogeochemical fluxes (Moreau et al., 2017; Frenger et al, 2018; Orselli et al., 2019; Rohr et al., 2020a-b, Patel et al., 2020). An improved understanding of how fine scales distribute micronekton and mesozooplankton (the so-called *intermediate trophic levels*) is pivotal for building a comprehensive view of marine ecosystems, from phytoplankton all the way to top predators, as well as their role on exporting carbon into the deep ocean (Belcher et al, 2019, Davison et al, 2013).

In the North Atlantic, a handful of studies observed how eddies impact the distribution of micronekton using both midwater trawls and acoustic backscattering (Boyd et al. 1986; Craddock et al., 1992; Godø et al., 2012; Fennel and Rose, 2015; Della Penna and Gaube, 2020; Devine et al., 2021). In this region, eddies differed in micronekton abundances, community composition and patterns in acoustic backscattering from their surrounding waters. A growing number of studies are addressing the distribution of acoustic backscattering in the Southern Ocean, either to relate observed patterns to hydrographic features (Behagle et al., 2017; Escobar-Flores et al. 2018) or to define the boundaries of mesopelagic biogeographies (Proud et al., 2015). However, to our knowledge, no study has explicitly addressed how Southern Ocean mesoscale eddies affect the distribution of acoustic backscattering associated with micronekton.

Here, we combine hydrographical and acoustic measurements to analyze how a Southern Ocean cyclonic eddy affected acoustic backscattering vertically integrated over the upper 1,200 m, as well as its impact on the distribution of DSL. First, we highlight the contrasting distributions of DSL inside the eddy core with the surrounding waters from the case study of a transect. We relate some of these differences with gradients in the underwater light field and light attenuation properties in the water column. Second, we show how the integrated distribution of acoustic backscattering in the water column within the eddy core relates to ambient SAZ waters and the waters in the PFZ where the eddy formed. Finally, we discuss how the provenance of the eddy influences the resident micronekton. Specifically, while the eddy core displays micronekton acoustical properties that are more similar to its origin, the waters at the eddy periphery display more similarities to the SAZ, suggesting that the resident mesopelagic communities are mixed – at the eddy margins - with those from the SAZ.

2 Materials and Methods

2.1 Multi-platform sampling of the eddy and its region

The studied Southern Ocean cyclonic feature was tracked using satellite data (altimetry-derived Sea Surface Height and Sea Level Anomaly (SLA), Sea Surface Temperature, and near-surface chlorophyll) and sampled during the voyage IN2016_V02 of the Australian *RV Investigator* (Patel et al., 2019). In particular, we used SLA maps to track and illustrate the position and shape of the eddy (Fig.1). SLA data were downloaded from the Copernicus CMEMS web portal as daily maps gridded to a nominal spatial resolution of ¼°. The studied eddy had been first

identified as a meander in the Sub-Antarctic Front (SAF) on 3 February 2016 that then detached as a cyclonic eddy and started moving northward on 3 March 2016 (Patel et al., 2019). The eddy had a diameter of approximately 190 km and was sampled between the 30 March and 5 April 2016, approximately 20 days before the eddy was re-absorbed by a SAF meander.

After sampling the eddy with a star-shaped pattern of Conductivity-Temperature-Depth (CTD) stations (Fig. 1), the *RV Investigator* headed to the PFZ, where the eddy had originated 27 days before the beginning of our sampling (Moreau et al., 2017; Patel et al., 2019). The PFZ and the SAF were observed for ~ 18 hours before the *RV Investigator* headed back towards port in Hobart, Tasmania, allowing for some more sampling of the SAZ in the proximity of the eddy.

Physical, biological, biogeochemical, and acoustic measurements were performed inside the eddy, in the surrounding SAZ and in the PFZ. Continuous sampling with a thermosalinograph, an in-line fluorometer, and 18 CTD casts revealed a marked doming of isopycnals as well as anomalies in temperature, oxygen distribution, salinity, chlorophyll and nutrients inside the eddy (Moreau et al., 2017; Patel et al., 2019; Patel et al.,2020). The onboard 75 kHz acoustic Doppler current profiler (ADCP) was used to identify the location of the eddy center following Patel et al. (2019) and to discriminate between the eddy core and periphery (in red and ochre respectively in Fig. S1). Here, we consider the eddy core as the region within 25 km from the eddy center, where geostrophic velocities near the surface were smaller than 30 cm/s (Patel et. al, 2019). We assume all observations within an anulus with radii of 25 km and 75 km away from the eddy center as belonging to the eddy periphery. *In situ* physical and biogeochemical measurements discussed by Moreau et al., (2017) were used to define the boundaries between the PFZ and the SAZ.

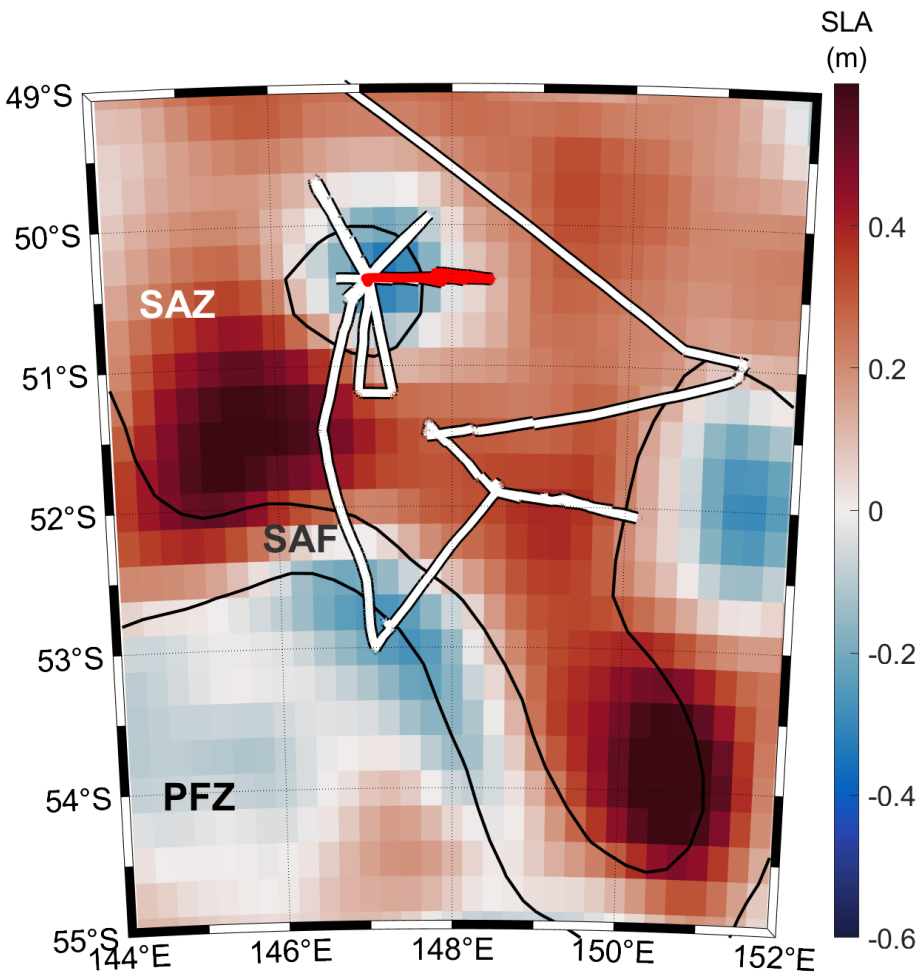

Figure 1 Map of Sea Level Anomaly (SLA, referring to 01/04/2016) for the region of interest. *Black contours indicate isolines of Sea Surface Height and identify the eddy and two branches of the Sub-Antarctic Front (SAF). White lines identify the ship track. The transect shown in Figure 2 corresponds to the part of the ship track marked in red.*

2.2 Acoustic measurements and processing

A single-beam scientific echosounder (*Simrad EK60, Kongsberg Maritime*) was used to measure acoustic volume backscattering (Sv dB re 1 m^{-1}) during the entire duration of the trip at the frequency of 18 kHz. Pulse length and pinging period were 2 ms and 0.2 Hz respectively. The echosounder was calibrated prior to the voyage and we assume no change in the Sv calibration with surface temperature as sound velocity induced variations cancel out (Bodholt, 2002). Since our study is focused on comparing patterns in the distribution of Sv, any bulk echosounder performance change should not impair the analysis of the gradients we present. In total, we collected more than 308 hours of acoustic data, 159 during daytime and 149 during night-time: 62 hours inside the eddy core (42 daytime/20 night-time), 55 hours within the periphery of the eddy (23/32), 173 hours in the SAZ (82/91) and 18 hours in the PFZ and SAF (12/6, Table 1).

Daytime and night-time observations were classified by comparing the time-stamp associated with each ping with the sunrise and sunset times computed for the associated longitude and latitude calculated using the equations described in Meus et al., (1991). Observations collected within 30 minutes of sunrise and sunset were excluded for the average daytime or night-time profiles and only retained to plot the echograms (Bianchi and Mislan, 2016). Raw data of backscattered power were processed using ESP3, an open-source software, Matlab-based package for visualizing and processing acoustics data, developed by the deepwater fisheries acoustics team at NIWA (Wellington, New Zealand, https://sourceforge.net/projects/esp3/, Ladroit et al., 2020). We assumed a sound speed of 1500 m/s and an absorption coefficient of 0.0027 m^{-1}. Data were processed using the software bad data detection, spike detection, and noise filtering algorithms (with a noise threshold of -140 dB, spike threshold of 10 dB). No corrections were made for non-linear power responses as outlined by De Robertis et al., (2019) as our results are treated as relative indicators and were not used to calculate fish biomass. Observations from depths below 1,200 m and shallower than 15 m were excluded from this analysis since the corresponding signal tends to be dominated by noise or the waves and bubbles near the surface. Nautical area scattering coefficients (NASC) were calculated using the equations detailed in MacLennan, (2002) over depth intervals of 5m. NASC is commonly used in fisheries acoustics to represent the linear increase in the numbers of biomass of fish present of similar size/weight and acoustic reflectivity.

	Eddy core	**Eddy periphery**	**SAZ**	**PFZ**
Daytime	40	23	82	12
Night-time	20	32	91	6
Total	62	55	173	18

Table 1: Duration of sampling *in hours for the different subregions explored during IN2016_V02*

2.3 Estimates of underwater light-levels and near-surface fluorescence

We used vertical profiles of photosynthetically available radiation (PAR) to estimate the vertical distribution of irradiance and describe the light levels encountered by the mesopelagic organisms in the different sampled subregions. Daytime CTD casts with PAR measurements were obtained from the subregions as follows: 4 in the eddy core, 4 at the periphery, 3 in the SAZ and 2 in the PFZ. Since the light levels that characterize the mesopelagic are below the detection limit of the PAR sensor (Log Quantum Cosine Irradiance Sensor, QCP2300, Biospherical), we estimated a representative coefficient of diffuse light attenuation, k_d(PAR), for each subregion. Daytime observations of PAR between 50-180m were used to fit a linear relationship between log(PAR) and depth (Fig. S2 in the Supplementary Materials). These k_d(PAR) values were used to estimate the average profiles of irradiance for each subregion and compared using a Student's *t* test.

In the transition between subregions, we used uncalibrated measurements of fluorescence of near-surface water sampled through the shipboard flow-through system using a WETStar fluorometer (WS3S-443P, Wetlabs, SeaBird Inc.). As detailed in Moreau et al., (2017), these fluorescence measurements were impacted by differences in the fluorescence yield per unit

chlorophyll during different times of the day. However, the observations still produced a meaningful and consistent quantification of near-surface chlorophyll. We chose to use fluorescence to identify the strong gradient in near-surface chlorophyll associated with the periphery of the sampled eddy.

2.4 Historical acoustics observations of the Southern Ocean

To provide context for our acoustics observations, we integrated into our study a collection of acoustic observations collected by research vessels and ships of opportunity from the Integrated Marine Observing System (IMOS) / Australian Ocean Data Network (AODN, https://portal.aodn.org.au/). This dataset contains processed acoustic backscattering (S_v) that has been filtered for different types of noise following the guidelines described in Kunnath et al. (2021). From this relatively large dataset, we selected only the observations collected at 18 kHz during the summer-fall months (January-May), which restricted the dataset to ten voyages and corresponded to more than 700 hours of sampling (Table S1, Fig. S4). We then separated the observations obtained in the SAZ from the ones collected south of the SAF (in the PFZ). The SAF was defined using the 0.2 m isoline of Sea Surface Height following Sokolov and Rintoul (2009). To homogenize the sampling frequencies for the voyages, all acoustics observations were interpolated at 30 minutes' intervals.

3 Results

The vertical distribution of DSL inside the eddy core were remarkably different compared to the surrounding SAZ waters (Fig.2). The example in Fig.2 showcases observations of acoustic backscattering sampled while the *RV Investigator* was transiting from the core of the eddy to the ambient SAZ waters. As the vessel's distance from the eddy center approached 25 km (blue line in Fig. 2b), patterns in the distribution of acoustic backscattering changed dramatically (~3:00 a.m. UTC/ 13:00 local time, white dashed line in Fig. 2a and black line in Fig. 2b).

The depths of several DSL that are present both inside the eddy core and at the periphery were remarkably different in these two subregions (Fig. 2a). For instance, the deepest scattering layer in the core shoaled from ~ 1200m to 900m as the distance from the center increased, while the lower limit of the non-migrating DSL became ~ 100 m shallower. The upper limit of the non-migrating DSL also moved up in the water column as the ship transited outside of the eddy core. The general movement of all DSLs towards shallower depths correlated with the uplift of isolumes (depths characterized by the same light levels, dotted black lines in Fig. 2a). The latter was in turn linked to higher surface chlorophyll outside the eddy, which enhanced light's attenuation and reduced light's penetration into the water column (Fig. 2b). Light attenuation coefficients in the eddy core were significantly different from those of the eddy periphery ($p<0.05$), and surrounding SAZ waters ($p<0.05$), yet not significantly different ($p=0.07$) from the origin PFZ waters (Fig. S3).

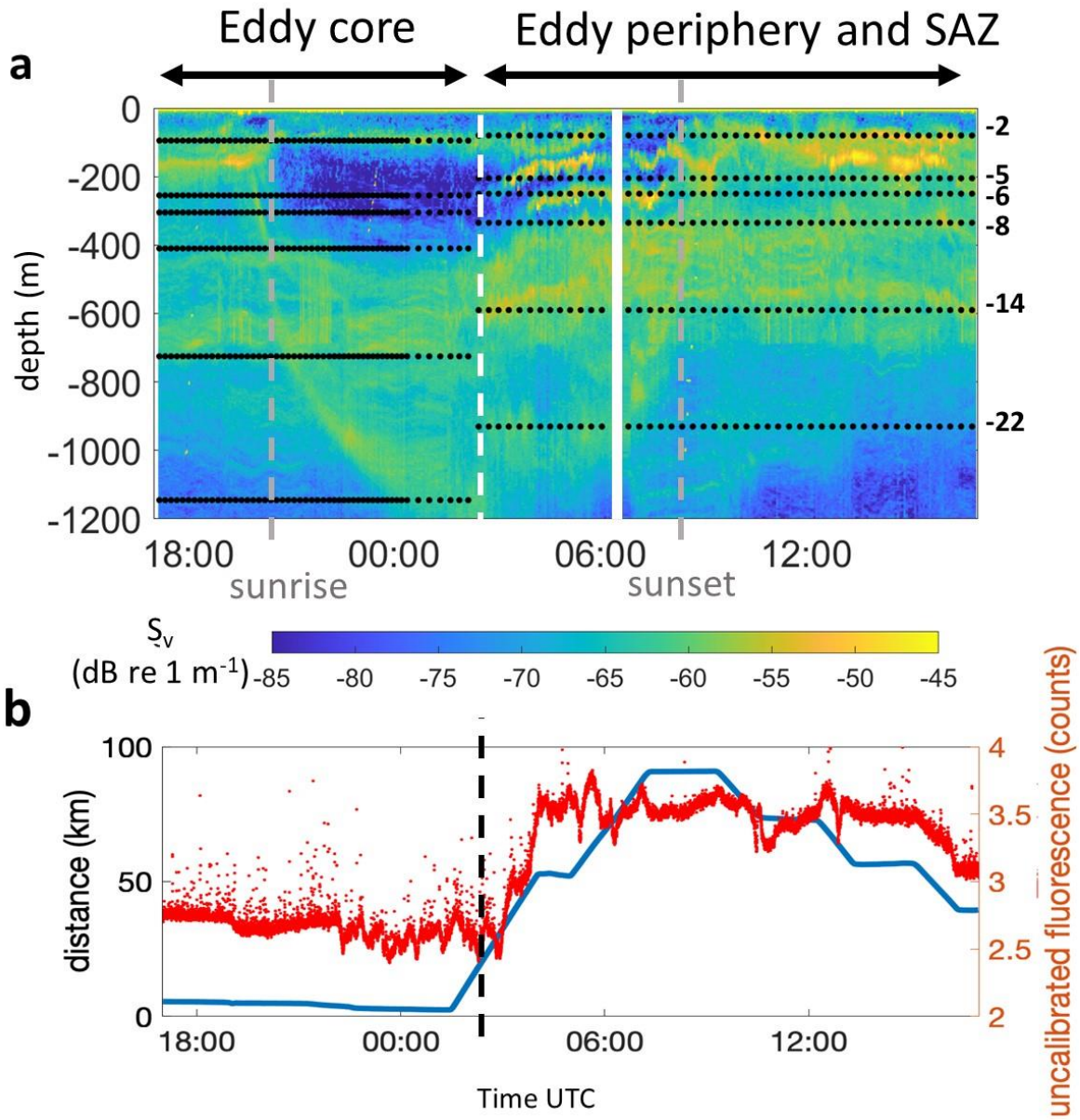

Figure 2 Echogram (a) showcasing an example of transition between eddy core (18:00-03:00 UTC / 04:00-13:00 local time) and eddy periphery (03:00-16:00 UTC / 13:00-02:00 local time). *This echogram refers to the time starting on 31/03/2016 UTC. Grey vertical dashed lines indicate the times corresponding to the DVM (towards and from the mesopelagic from left to right at approximately 20:00 UTC/ 06:00 local time and 08:00 UTC/18:00 local time, respectively) and the white dashed line represents the boundary between eddy core and periphery. White filled lines indicate data that was not retained during quality control. Horizontal dash lines represent the position of the isolumes for the eddy core and eddy periphery calculated from the CTD casts conducted in the respective regions. Different labeled isolumes represent how much of the light available near the surface penetrates to a given depth, in log10 scale.. As the distance from the eddy center increases (b, blue line), the boundary of the eddy*

core is crossed around 25 km away from its center and a sharp gradient in surface fluorescence appears (red dots in b).

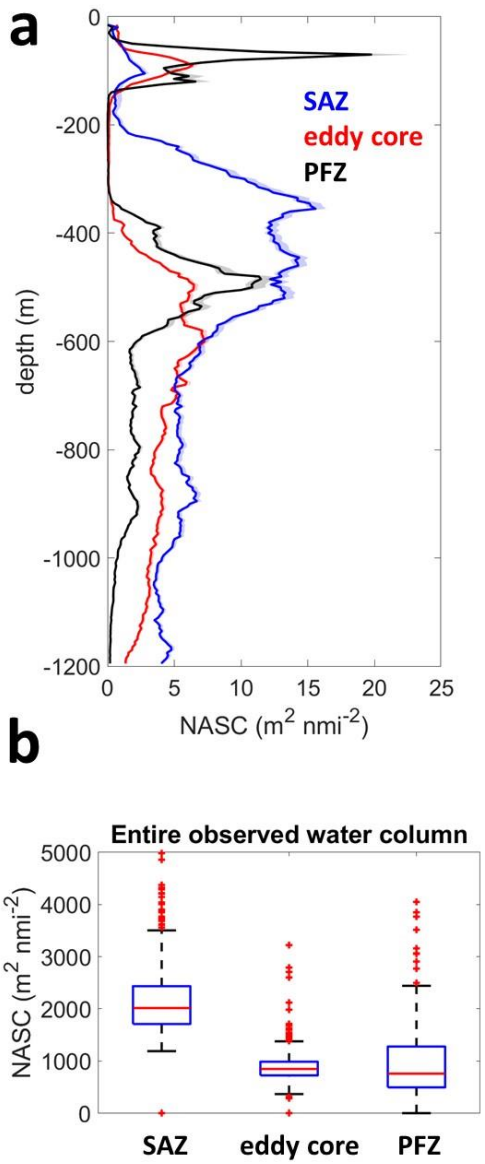

Figure 3 Differences in the distribution of deep scattering layers (DSLs, a) and integrated NASC *(b) between locations in the eddy core, in the Sub-Antarctic Zone (SAZ) and in the Polar Front Zone (PFZ). Solid lines in (a) indicate the median daytime NASC values in the SAZ (blue), in the eddy core (red), and in the PFZ (black). Shadings indicate the 25th and 75th percentiles divided by the square root of the number of observations.*

While differences in the light field account for some of the differences between the DSLs distribution in the eddy core and ambient waters, some scattering layers, such as those at 200-300 m were observed immediately outside of eddy, but not inside the eddy core. In contrast, the

100m deep scattering layer in the eddy core was not detected at 75 km from the center of the eddy.

On average, there were fewer and less acoustically reflective DSL in the eddy core compared to the SAZ waters (Fig.3a, Fig. S5). The average integrated NASC inside the core of the eddy was approximately 50% of the NASC in the surrounding waters of the SAZ (Fig. 3a, 3b and Fig. S6). By contrast, the daytime distribution of NASC in the top 600 m (corresponding to the epipelagic and upper mesopelagic) was remarkably similar to the PFZ, where the eddy had originated (Fig.3a). Integrated values of NASC in the PFZ were also as low as the inside the eddy core and noticeably smaller than the SAZ (Fig. 3b). This strong difference in acoustic backscattering between the SAZ and the PFZ was consistently found in historical acoustic data where integrated NASC values in the SAZ can be more than three times higher than in the PFZ (Fig. S4).

NASC differences between the eddy core and those in the PFZ are less than half of the differences between the eddy core and the SAZ (Fig.4). Observations of NASC from the eddy periphery were highly variable (ochre shading in Fig. 4,a) and, on average, intermediate between the SAZ and the eddy core ones (Fig. 4a). Conversely, NASC values measured at the eddy periphery are on average larger than the PFZ (positive anomalies in Fig. 4,b) throughout the water column.

4 Discussions and conclusions

We examined the distribution of acoustic backscattering inside the core and at the periphery of a cyclonic eddy and compared it with the typical patterns in acoustic backscattering in the SAZ and in the PFZ. Our major findings, which we explore here in more detail, were as follows. First, the distribution of DSL inside the eddy core was different from the ambient waters of the SAZ even a month after eddy formation. Differences were partially, yet not exclusively, due to changes in the light-field encountered by mesopelagic organisms due to the different horizontal distribution of near-surface phytoplankton. The average water-column integrated values of NASC inside the eddy core are similar to the average of the PFZ (950 m^2nmi^{-2} vs 850 m^2nmi^{-2}), but lower approximately 50% of the SAZ mean (Fig. 3). Finally, the eddy periphery values of acoustic backscattering were intermediate between those observed in the core and the SAZ ambient waters (Fig. 4).

Inside the eddy light penetrated deeper into the water column due to low concentrations of surface chlorophyll (Fig. 2b and Moreau et al., 2017). We estimated very low light attenuation coefficients typical of the Southern Ocean during autumn and winter (Nelson and Smith, 1991; Son and Wang, 2015). We did find statistically significant differences in light attenuation coefficients between the eddy core and the PFZ (low chlorophyll, clearer waters), the SAZ (higher chlorophyll), and the eddy periphery (also higher chlorophyll, higher light attenuation coefficient; Fig. S2). These differences affected the vertical distribution of DSL that, consistent with previous studies, matched the distribution of isolumes across the water column (Røstad et al., 2016, Aksnes et al., 2017). The horizontal gradients in the depths of DSL were sharp and matched the gradients in near-surface fluorescence that characterized the transition between the

core and the ambient waters of the SAZ, similar to other ocean basins (Della Penna and Gaube, 2020).

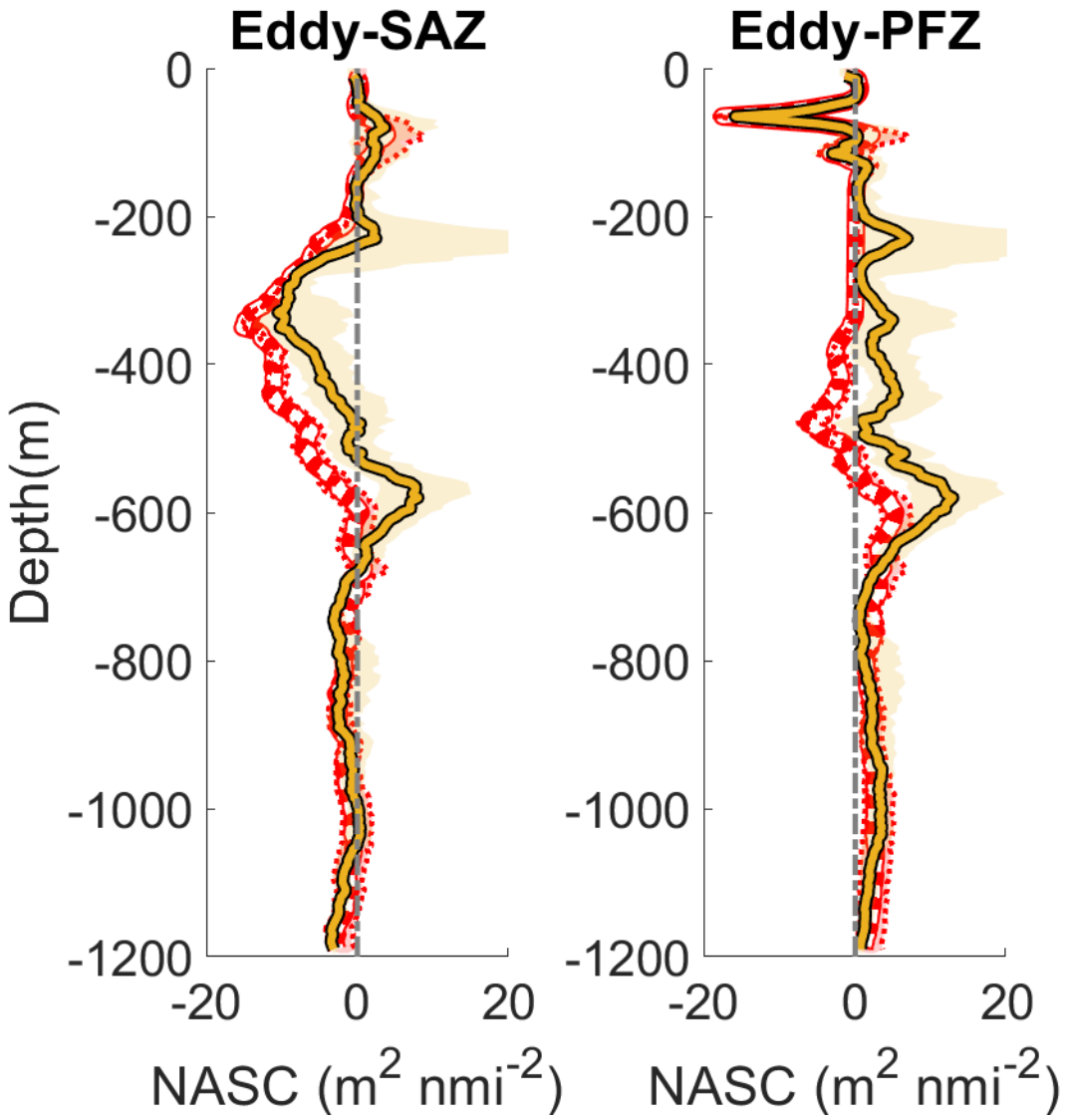

Figure 4 Differences between acoustic backscattering in selected areas of the eddy *(core in red/dashed line, periphery in yellow/ brown), the Sub Antarctic Zone (SAZ, a), and the Polar Front Zone (PFZ, b) as a function of depth. Shadings refer to the 25th-75th percentiles of the differences between the profiles from the eddy core and periphery compared to the median profiles of the SAZ and PFZ respectively.*

We observed a different number of DSL in the eddy core, with a deeper vertical distribution compared to ambient waters. Indeed, the distribution was more similar to the PFZ where the eddy originated. In particular, the eddy core retained some acoustic properties typical of its origin suggesting that micronekton were transported from the PFZ more than 200 km north in the SAZ, probably by eddy trapping. High to mid-latitude mesoscale eddies are characterized by a

trapping power due to their non-linearity (Early et al., 2011). Southern Ocean eddies have been suggested to trap, retain, and transport water parcels inside their cores (d'Ovidio et al., 2013). Our eddy had rotational speed averages of ~40 km/day and a translational speed between 1.5-6.6 km/day (1.7 km/day at the time of sampling, and maxima of 6.6 km/day when detaching from the meander, Patel et al., 2019). Therefore, the ratio between rotational speed and translational speed was > 5 for the entire lifetime of the eddy, suggesting that this eddy was highly nonlinear, with a strong trapping power (Chelton et al., 2011).

Eddy trapping has significant consequences for the transport of salt and heat across the Antarctic Circumpolar Current (Patel et al., 2019), impacts the distribution of primary producers (Dawson et al., 2018; Frenger et al., 2018), weather (Frenger et al., 2013), and regulates the exchanges of carbon crucial for climate (Moreau et al., 2017, Dufour et al, 2015). Our results show that eddy trapping also impacts mesopelagic micronekton. It is difficult to evaluate whether micronekton alone were trapped and transported or if it was their zooplanktonic prey that was transported and the micronekton followed. Without complementary observations of zooplankton and micronekton community composition, it is not possible to provide a definitive answer to this question. However, two lines of evidence suggest that micronekton itself was trapped and transported. First, studies focused on trawl and predator avoidance suggest that most mesopelagic micronekton are generally lethargic when not vertically migrating or actively escaping from a threat (Kaartvedt et al., 2012). Second, to initiate movement, it is likely that micronekton would be responding to a stimulus, such as a gradient in temperature, pressure or light (Franks, 1992). From the inner core of a mesoscale eddy, the closest horizontal gradients in such properties (orders of magnitude weaker than the vertical ones) are tens of kilometers away requiring for a mesopelagic fish to be able to perceive a gradient on scales that are four orders of magnitudes larger than their body size.

Our results also indicate that, while the eddy core preserved many of the acoustical properties of the PFZ, the structure of DSL in the eddy periphery was more similar to the SAZ. We can interpret this pattern as an indicator of exchanges and mixing of water parcels (and the organisms there contained) between the SAZ and the periphery of the eddy. This result is supported by the analysis of water masses conducted using CTD data collected during the same voyage (Moreau et al., 2017) and by the overall distribution of biogeochemical tracers (Patel et al., 2020) including oxygen (Fig. S7). These findings are consistent with the theoretical results about eddy trapping by Early et al. (2011), who highlighted that while eddy core waters can be ``isolated'' for a significant part of an eddy lifetime, the peripheries of eddies regularly exchange water masses with the surroundings.

The strong difference between the SAZ and PFZ observed during INV2016_V02, both in terms of integrated NASC, and distribution of DSL, was corroborated by the historical data from the IMOS database, that consistently show less acoustic backscattering in the PFZ compared to the SAZ. This was also shown in other studies that have found a general decrease in acoustic backscattering with increased latitude (Escobar-Flores et al., 2018; Dornan et al., 2019).

The depth of DSL located at ~ 100m matches the mixed layer depth and the beginning of the thermocline as well as a peak in the vertical distribution of ammonia that can reflect excretion by

marine organism such as zooplankton and fish (Patel et al., 2019). While changes in density associated with the upper thermocline have been observed with 18 kHz echo-sounding (Stranne et al., 2018), the high values of acoustic backscattering associated with this DSL are spread over a depth range of more than 50m suggesting that they are more likely associated with a biological signal.

Acoustic backscattering is commonly used as a fisheries-independent way to estimate fish biomass (Fernandes et al., 2002; Kloser et al., 2009; Irigoien et al., 2014). Our main conclusion is that the sampled cyclonic eddy had lower mesopelagic micronekton biomass compared to the ambient SAZ waters and similarly to its origin on the PFZ. However, we should consider alternative explanations for our observations. A recent study by Dornan et al., (2019) showed that fish biomass estimated with acoustic backscattering decreased with increasing latitude in the Southern Ocean, whereas biomass measured using mid-water trawls did not. This trend was attributed to size and physiological temperature-driven changes in the resonating swim-bladders that are responsible of strong backscattering signal. We think it is unlikely that the small temperature and latitude difference between the eddy location in the SAZ and its SAF origin are responsible for the observed differences. Another possibility is a change in community composition of the micronekton: some species of micronekton do not have a swim-bladder or it is filled with oil instead of air, causing weaker backscattering signals. This may have impacted our results if the community composition was different in the SAZ compared to the SAF, but this is part of our point: the eddy transported the community from its origin to where we sampled it. Finally, fish belonging to the same species, but characterized by different size (and therefore of a larger or smaller swim bladder) can backscatter sound differently producing different profiles of acoustic backscattering (Fielding et al., 2012). During the IN2016_V02 expedition, we did not carry out any mid-water trawling, and, therefore, we cannot discriminate further all aspects of these hypotheses. However, our results suggest a difference between an eddy and the surrounding waters in terms of biomass, community composition and/or physiological state. Future studies will be needed to understand how these effects intertwine with each other and affect the patchiness of micronekton distribution, eventually impacting the foraging strategies of top predators.

Differences in the horizontal and vertical distribution of mesopelagic micronekton can have important consequences for upper trophic levels. In the region of interest, the organisms inhabiting the DSL we detected typically include myctophids, squids, swarming euphasiids, and amphipods (Flynn and Kloser, 2012). These animals constitute the prey of a variety of marine megafauna, including seabirds, penguins, and marine mammals (Cherel et al., 2010; Watanuki and Thiebot, 2018; McMahon et al., 2019). For these diving predators, horizontal patchiness of their prey field is an important driver of their foraging strategies, so differences in micronekton composition or abundance can underpin their interactions with the prey fields which are in turn set by the dynamics associated with mesoscale eddies. Furthermore, the differences in vertical distribution of DSL are likely to have an impact on the accessibility of the prey to diving predators. This difference might be particularly dramatic for air-breathing animals such as seabirds and marine mammals whose foraging time underwater is limited by the need to breathe at the surface (Jaud et al., 2012; Guinet et al., 2014; O'Toole et al., 2017), but also to fish whose thermal niche can limit the vertical extent of their diving behavior (Gaube et al., 2018; Braun et al., 2019). In general, the metabolic cost associated with getting the same amount of energy if the

prey is located deeper in the water column (and therefore potentially in colder water) will be higher. These costs have the potential to result in cyclonic eddies, like the one we sampled, being a non-profitable region for foraging.

Acknowledgments

We would like to thank the Captain, the crew, and the technicians and scientists onboard of the IN2016_V02 voyage. This study has been conducted using E.U. Copernicus Marine Service Information (CMEMS). This research was supported under Australian Research Council's Special Research Initiative for Antarctic Gateway Partnership (Project ID SR140300001), by the Australian Research Council Discovery Grant DP160102870, the ARC Centre of Excellence for Climate System Science (CE1101028) and ship time from Australia's Marine National Facility. In addition, Joan Llort was supported by the European Union's Horizon 2020 research and innovation programme under the Marie Skłodowska-Curie grant agreement No. 754433. All data from the underway system and the echosounder are available at https://portal.aodn.org.au/search and https://www.marine.csiro.au/data/trawler/survey_details.cfm?survey=IN2016_V02. Data was sourced from the Integrated Marine Observing System (IMOS) - an initiative of the Australian Government being conducted as part of the National Collaborative Research Infrastructure Strategy and the Super Science Initiative. IMOS is operated by a consortium of institutions as an unincorporated joint venture, with the University of Tasmania as Lead Agent.

References

Aksnes, D. L., Røstad, A., Kaartvedt, S., Martinez, U., Duarte, C. M., & Irigoien, X. (2017). Light penetration structures the deep acoustic scattering layers in the global ocean. *Science advances*, *3*(5), e1602468. https://doi.org/10.1126/sciadv.1602468

Belcher, A., Saunders, R.A., Tarling, G.A., 2019. Respiration rates and active carbon flux of mesopelagic fishes (Family Myctophidae) in the Scotia Sea, Southern Ocean. Marine Ecology Progress Series 610, 149–162. https://doi.org/10.3354/meps12861

Bianchi, D., Stock, C., Galbraith, E. D., & Sarmiento, J. L. (2013). Diel vertical migration: Ecological controls and impacts on the biological pump in a one-dimensional ocean model. *Global Biogeochemical Cycles*, *27*(2), 478-491. https://doi.org/10.1002/gbc.20031

Bianchi, D., & Mislan, K. A. S. (2016). Global patterns of diel vertical migration times and velocities from acoustic data. *Limnology and Oceanography*, *61*(1), 353-364. https://doi.org/10.1002/lno.10219

Bailleul, F., Cotté, C., & Guinet, C. (2010). Mesoscale eddies as foraging area of a deep-diving predator, the southern elephant seal. *Marine Ecology Progress Series*, *408*, 251-264. https://doi.org/10.3354/meps08560

Béhagle, N., Cotté, C., Lebourges-Dhaussy, A., Roudaut, G., Duhamel, G., Brehmer, P., ... & Cherel, Y. (2017). Acoustic distribution of discriminated micronektonic organisms from a bi-

frequency processing: the case study of eastern Kerguelen oceanic waters. *Progress in Oceanography*, *156*, 276-289. https://doi.org/10.1016/j.pocean.2017.06.004

Bodholt, H., 2002, June. The effect of water temperature and salinity on echo sounder measurements. In *ICES Symposium on Acoustics in Fisheries* (pp. 1-7).

Bost, C. A., Cotté, C., Bailleul, F., Cherel, Y., Charrassin, J. B., Guinet, C., ... & Weimerskirch, H. (2009). The importance of oceanographic fronts to marine birds and mammals of the southern oceans. *Journal of Marine Systems*, *78*(3), 363-376. https://doi.org/10.1016/j.jmarsys.2008.11.022

Boyd, S. H., Wiebe, P. H., Backus, R. H., Craddock, J. E., & Daher, M. A. (1986). Biomass of the micronekton in Gulf Stream ring 82-B and environs: changes with time. *Deep Sea Research Part A. Oceanographic Research Papers*, *33*(11-12), 1885-1905. https://doi.org/ 10.1016/0198-0149(86)90084-1

Braun, C. D., Gaube, P., Sinclair-Taylor, T. H., Skomal, G. B., & Thorrold, S. R. (2019). Mesoscale eddies release pelagic sharks from thermal constraints to foraging in the ocean twilight zone. *Proceedings of the National Academy of Sciences*, *116*(35), 17187-17192. https://doi.org/10.1073/pnas.1903067116

Chapman, C. C., Lea, M. A., Meyer, A., Sallée, J. B., & Hindell, M. (2020). Defining Southern Ocean fronts and their influence on biological and physical processes in a changing climate. *Nature Climate Change*, 1-11. https://doi.org/10.1038/s41558-020-0705-4

Chelton, D.B., Schlax, M.G. and Samelson, R.M., 2011. Global observations of nonlinear mesoscale eddies. *Progress in oceanography*, *91*(2), pp.167-216. https://doi.org/10.1016/j.pocean.2011.01.002

Cherel, Y., Fontaine, C., Richard, P., & Labatc, J. P. (2010). Isotopic niches and trophic levels of myctophid fishes and their predators in the Southern Ocean. *Limnology and oceanography*, *55*(1), 324-332. https://doi.org/10.4319/lo.2010.55.1.0324

Cotté, C., Park, Y. H., Guinet, C., & Bost, C. A. (2007). Movements of foraging king penguins through marine mesoscale eddies. *Proceedings of the Royal Society B: Biological Sciences*, *274*(1624), 2385-2391. https://doi.org/10.1098/rspb.2007.0775

Cotté, C., d'Ovidio, F., Dragon, A. C., Guinet, C., & Lévy, M. (2015). Flexible preference of southern elephant seals for distinct mesoscale features within the Antarctic Circumpolar Current. *Progress in Oceanography*, *131*, 46-58. https://doi.org/10.1016/j.pocean.2014.11.011

Craddock, J. E., Backus, R. H., & Daher, M. A. (1992). Vertical distribution and species composition of midwater fishes in warm-core Gulf Stream meander/ring 82-H. *Deep Sea Research Part A. Oceanographic Research Papers*, *39*, S203-S218. https://doi.org/10.1016/S0198-0149(11)80012-9

Cuvier, G. *Le Règne Animal distribué d'après son Organisation pour à l'Histoire Naturelle des Animaux et d'Introduction à l'Anatomie Compare* (Deterville, 1817).

d'Ovidio, F., De Monte, S., Della Penna, A., Cotté, C., & Guinet, C. (2013). Ecological implications of eddy retention in the open ocean: a Lagrangian approach. *Journal of Physics A: Mathematical and Theoretical*, *46*(25), 254023. https://doi.org/ 10.1088/1751-8113/46/25/254023

Davison, P.C., Checkley, D.M., Koslow, J.A., Barlow, J., 2013. Carbon export mediated by mesopelagic fishes in the northeast Pacific Ocean. Progress in Oceanography 116, 14–30. https://doi.org/10.1016/j.pocean.2013.05.013

Dawson, H. R., Strutton, P. G., & Gaube, P. (2018). The unusual surface chlorophyll signatures of Southern Ocean eddies. *Journal of Geophysical Research: Oceans*, *123*(9), 6053-6069. https://doi.org/10.1029/2017JC013628

De Robertis, A., Bassett, C., Andersen, L.N., Wangen, I., Furnish, S. and Levine, M., 2019. Amplifier linearity accounts for discrepancies in echo-integration measurements from two widely used echosounders. *ICES Journal of Marine Science*, *76*(6), pp.1882-1892. https://doi.org/10.1093/icesjms/fsz040

Della Penna, A., De Monte, S., Kestenare, E., Guinet, C., & d'Ovidio, F. (2015). Quasi-planktonic behavior of foraging top marine predators. *Scientific reports*, *5*(1), 1-10. https://doi.org/10.1038/srep18063

Della Penna, A., Gaube, P., (2020). Mesoscale eddies structure mesopelagic communities. *Frontiers in Marine Science* https://doi.org/10.3389/fmars.2020.00454

Devine, B., Fennell, S., Themelis, D. and Fisher, J.A., (2021). Influence of anticyclonic, warm-core eddies on mesopelagic fish assemblages in the Northwest Atlantic Ocean. *Deep Sea Research Part I: Oceanographic Research Papers*, p.103555. http://doi.org/*10.1016/j.dsr.2021.103555*

Dornan, T., Fielding, S., Saunders, R. A., & Genner, M. J. (2019). Swimbladder morphology masks Southern Ocean mesopelagic fish biomass. *Proceedings of the Royal Society B*, *286*(1903), 20190353. https://doi.org/10.1098/rspb.2019.0353

Dragon, A. C., Monestiez, P., Bar-Hen, A., & Guinet, C. (2010). Linking foraging behaviour to physical oceanographic structures: Southern elephant seals and mesoscale eddies east of Kerguelen Islands. *Progress in Oceanography*, *87*(1-4), 61-71. https://doi.org/10.1016/j.pocean.2010.09.025

Dufour, C. O., Griffies, S. M., de Souza, G. F., Frenger, I., Morrison, A. K., Palter, J. B., ... & Slater, R. D. (2015). Role of mesoscale eddies in cross-frontal transport of heat and biogeochemical tracers in the Southern Ocean. *Journal of Physical Oceanography*, *45*(12), 3057-3081. https://doi.org/10.1175/JPO-D-14-0240.1

Early, J. J., Samelson, R. M., & Chelton, D. B. (2011). The evolution and propagation of quasigeostrophic ocean eddies. *Journal of Physical Oceanography*, *41*(8), 1535-1555. https://doi.org/10.1175/2011JPO4601.1

Escobar-Flores, P. C., Driscoll, R. L., & Montgomery, J. C. (2018). Spatial and temporal distribution patterns of acoustic backscatter in the New Zealand sector of the Southern Ocean. *Marine Ecology Progress Series*, *592*, 19-35. https://doi.org/10.3354/meps12489

Fennell, S., & Rose, G. (2015). Oceanographic influences on deep scattering layers across the North Atlantic. *Deep Sea Research Part I: Oceanographic Research Papers*, *105*, 132-141. https://doi.org/10.1016/j.dsr.2015.09.002

Fernandes, P. G., Gerlotto, F., Holliday, D. V., Nakken, O., & Simmonds, E. J. (2002). Acoustic applications in fisheries science: the ICES contribution. ICES.

Fielding, S., Watkins, J. L., Collins, M. A., Enderlein, P., & Venables, H. J. (2012). Acoustic determination of the distribution of fish and krill across the Scotia Sea in spring 2006, summer 2008 and autumn 2009. *Deep Sea Research Part II: Topical Studies in Oceanography*, *59*, 173-188. https://doi.org/10.1016/j.dsr2.2011.08.002

Flynn, A. J., & Kloser, R. J. (2012). Cross-basin heterogeneity in lanternfish (family Myctophidae) assemblages and isotopic niches (δ13C and δ15N) in the southern Tasman Sea abyssal basin. *Deep Sea Research Part I: Oceanographic Research Papers*, *69*, 113-127. https://doi.org/10.1016/j.dsr.2012.07.007

Franks, P. J. (1992). Sink or swim: Accumulation of biomass at fronts. *Marine ecology progress series. Oldendorf*, *82*(1), 1-12. https://doi.org/10.3354/meps082001

Frenger, I., Gruber, N., Knutti, R., & Münnich, M. (2013). Imprint of Southern Ocean eddies on winds, clouds and rainfall. *Nature geoscience*, *6*(8), 608-612. https://doi.org/10.1038/ngeo1863

Frenger, I., Münnich, M., & Gruber, N. (2018). Imprint of Southern Ocean eddies on chlorophyll. *Biogeosciences (BG)*, *15*, 4781-4798. https://doi.org/10.5194/bg-15-4781-2018

Gaube, P., Braun, C. D., Lawson, G. L., McGillicuddy, D. J., Della Penna, A., Skomal, G. B., ... & Thorrold, S. R. (2018). Mesoscale eddies influence the movements of mature female white sharks in the Gulf Stream and Sargasso Sea. *Scientific reports*, *8*(1), 1-8. https://doi.org/10.1038/s41598-018-25565-8

Godø, O. R., Samuelsen, A., Macaulay, G. J., Patel, R., Hjøllo, S. S., Horne, J., ... & Johannessen, J. A. (2012). Mesoscale eddies are oases for higher trophic marine life. *PloS one*, *7*(1). https://doi.org/10.1371/journal.pone.0030161

Greene, C. H., & Wiebe, P. H. (1990). Bioacoustical oceanography: new tools for zooplankton and micronekton research in the 1990s. *Oceanography*, *3*(1), 12-17. https://doi.org/10.5670/oceanog.1990.15

Guinet, C., Vacquié-Garcia, J., Picard, B., Bessigneul, G., Lebras, Y., Dragon, A. C., ... & Bailleul, F. (2014). Southern elephant seal foraging success in relation to temperature and light conditions: insight into prey distribution. *Marine Ecology Progress Series*, *499*, 285-301. https://doi.org/10.3354/meps10660

Hays, G. C. (2003). A review of the adaptive significance and ecosystem consequences of zooplankton diel vertical migrations. In *Migrations and Dispersal of Marine Organisms* (pp. 163-170). Springer, Dordrecht. https://doi.org/10.1023/B:HYDR.0000008476.23617.b0

Irigoien, X., Klevjer, T. A., Røstad, A., Martinez, U., Boyra, G., Acuña, J. L., ... & Agusti, S. (2014). Large mesopelagic fishes biomass and trophic efficiency in the open ocean. *Nature communications*, *5*(1), 1-10. https://doi.org/10.1038/ncomms4271

Jaud, T., Dragon, A. C., Garcia, J. V., & Guinet, C. (2012). Relationship between chlorophyll a concentration, light attenuation and diving depth of the southern elephant seal Mirounga leonina. *PLoS one*, *7*(10). https://doi.org/10.1371/journal.pone.0047444

Kaartvedt, S., Staby, A., & Aksnes, D. L. (2012). Efficient trawl avoidance by mesopelagic fishes causes large underestimation of their biomass. *Marine Ecology Progress Series*, *456*, 1-6. https://doi.org/10.3354/meps09785 https://doi.org/10.3354/meps09785

Klevjer, T. A., Irigoien, X., Røstad, A., Fraile-Nuez, E., Benítez-Barrios, V. M., & Kaartvedt, S. (2016). Large scale patterns in vertical distribution and behaviour of mesopelagic scattering layers. *Scientific reports*, *6*, 19873. https://doi.org/10.1038/srep19873

Kloser, R. J., Ryan, T. E., Young, J. W., & Lewis, M. E. (2009). Acoustic observations of micronekton fish on the scale of an ocean basin: potential and challenges. *ICES Journal of Marine Science*, *66*(6), 998-1006. https://doi.org/10.1093/icesjms/fsp077

Kloser, R. J., Ryan, T. E., Keith, G., & Gershwin, L. (2016). Deep-scattering layer, gas-bladder density, and size estimates using a two-frequency acoustic and optical probe. *ICES Journal of Marine Science*, *73*(8), 2037-2048. https://doi.org/10.1093/icesjms/fsv257

Kunnath, Haris., Kloser, R.J., Ryan, T.E., Downie, R.A., Keith, G. and Nau, A.W., 2021. Sounding out life in the deep using acoustic data from ships of opportunity. *Scientific Data*, *8*(1), pp.1-23. https://doi.org/10.1038/s41597-020-00785-8

Ladroit, Y., Escobar-Flores, P. C., Schimel, A. C., & O'Driscoll, R. L. (2020). ESP3: An open-source software for the quantitative processing of hydro-acoustic data. *SoftwareX*, *12*, 100581. https://doi.org/10.1016/j.softx.2020.100581

MacLennan, D. N., Fernandes, P. G., & Dalen, J. (2002). A consistent approach to definitions and symbols in fisheries acoustics. *ICES Journal of Marine Science*, *59*(2), 365-369. https://doi.org/10.1006/jmsc.2001.1158

McMahon, C. R., Hindell, M. A., Charrassin, J. B., Corney, S., Guinet, C., Harcourt, R., ... & Bestley, S. (2019). Finding mesopelagic prey in a changing Southern Ocean. *Scientific Reports*, *9*(1), 1-11. https://doi.org/10.1038/s41598-019-55152-4

Meeus, Jean H. Astronomical algorithms. Willmann-Bell, Incorporated, 1991.

Moreau, S., Della Penna, A., Llort, J., Patel, R., Langlais, C., Boyd, P. W., ... & Lenton, A. (2017). Eddy-induced carbon transport across the Antarctic Circumpolar Current. *Global Biogeochemical Cycles*, *31*(9), 1368-1386. https://doi.org/10.1002/2017GB005669

Morrow, R., Donguy, J. R., Chaigneau, A., & Rintoul, S. R. (2004). Cold-core anomalies at the subantarctic front, south of Tasmania. *Deep Sea Research Part I: Oceanographic Research Papers*, *51*(11), 1417-1440. https://doi.org/10.1016/j.dsr.2004.07.005

Murphy, E. J., Cavanagh, R. D., Drinkwater, K. F., Grant, S. M., Heymans, J. J., Hofmann, E. E., ... & Johnston, N. M. (2016). Understanding the structure and functioning of polar pelagic ecosystems to predict the impacts of change. *Proceedings of the Royal Society B: Biological Sciences*, *283*(1844), 20161646. https://doi.org/10.1098/rspb.2016.1646

Nelson, D.M. and Smith Jr, W.0., 1991. Sverdrup revisited: Critical depths, maximum chlorophyll levels, and the control of Southern Ocean productivity by the irradiance-mixing regime. *Limnology and Oceanography*, *36*(8), pp.1650-1661. https://doi.org/10.4319/lo.1991.36.8.1650

Orselli, I.B., Kerr, R., de Azevedo, J.L., Galdino, F., Araujo, M. and Garcia, C.A., 2019. The sea-air CO2 net fluxes in the South Atlantic Ocean and the role played by Agulhas eddies. *Progress in Oceanography*, *170*, pp.40-52. https://doi.org/10.1016/j.pocean.2018.10.006

O'Toole, M., Guinet, C., Lea, M. A., & Hindell, M. A. (2017). Marine predators and phytoplankton: how elephant seals use the recurrent Kerguelen plume. *Marine Ecology Progress Series*, *581*, 215-227. https://doi.org/10.3354/meps12312

Patel, R. S., Phillips, H. E., Strutton, P. G., Lenton, A., & Llort, J. (2019). Meridional Heat and Salt Transport Across the Subantarctic Front by Cold-Core Eddies. *Journal of Geophysical Research: Oceans*, *124*(2), 981-1004. https://doi.org/10.1029/2018JC014655

Patel, R. S., Llort, J., Strutton, P. G., Phillips, H. E., Moreau, S., Conde Pardo, P., & Lenton, A. The biogeochemical structure of Southern Ocean mesoscale eddies. *Journal of Geophysical Research: Oceans*, e2020JC016115. https://doi.org/10.1029/2020JC016115

Proud, R., Cox, M. J., & Brierley, A. S. (2017). Biogeography of the global ocean's mesopelagic zone. *Current Biology*, *27*(1), 113-119. https://doi.org/10.1016/j.cub.2016.11.003

Rohr, T., Harrison, C., Long, M. C., Gaube, P., & Doney, S. C. The simulated biological response to Southern Ocean eddies via biological rate modification and physical transport. *Global Biogeochemical Cycles*, e2019GB006385. https://doi.org/10.1029/2019GB006385

Rohr, T., Harrison, C., Long, M. C., Gaube, P., & Doney, S. C. Eddy-modified iron, light, and phytoplankton cell division rates in the simulated Southern Ocean. *Global Biogeochemical Cycles*, e2019GB006380. https://doi.org/10.1029/2019GB006380

Røstad, A., Kaartvedt, S., & Aksnes, D. L. (2016). Light comfort zones of mesopelagic acoustic scattering layers in two contrasting optical environments. *Deep Sea Research Part I: Oceanographic Research Papers*, *113*, 1-6. https://doi.org/10.1016/j.dsr.2016.02.020

Ryan, T. E., Kloser, R. J., & Macaulay, G. J. (2009). Measurement and visual verification of fish target strength using an acoustic-optical system attached to a trawlnet. *ICES Journal of Marine Science*, *66*(6), 1238-1244. https://doi.org/10.1093/icesjms/fsp122

Ryan, T. (2011). Overview of data collection, management and processing procedures of underway acoustic data. IMOS BASOOP sub-facility.

Son, S., & Wang, M. (2015). Diffuse attenuation coefficient of the photosynthetically available radiation Kd (PAR) for global open ocean and coastal waters. *Remote Sensing of Environment*, *159*, 250-258. https://doi.org/10.1016/j.rse.2014.12.011

Subramaniam, R. C., Corney, S. P., Swadling, K. M., & Melbourne-Thomas, J. (2020). Exploring ecosystem structure and function of the northern Kerguelen Plateau using a mass-balanced food web model. *Deep Sea Research Part II: Topical Studies in Oceanography*, 104787. https://doi.org/10.1016/j.dsr2.2020.104787

Stranne, C., Mayer, L., Jakobsson, M., Weidner, E., Jerram, K., Weber, T.C., Anderson, L.G., Nilsson, J., Björk, G. and Gårdfeldt, K., 2018. Acoustic mapping of mixed layer depth. *Ocean Science*, *14*(3), pp.503-514 https://doi.org/10.5194/os-14-503-2018

Tew-Kai, E., Rossi, V., Sudre, J., Weimerskirch, H., Lopez, C., Hernandez-Garcia, E., ... & Garçon, V. (2009). Top marine predators track Lagrangian coherent structures. *Proceedings of the National Academy of Sciences*, *106*(20), 8245-8250. https://doi.org/10.1073/pnas.0811034106

Urmy, S. S., & Horne, J. K. (2016). Multi-scale responses of scattering layers to environmental variability in Monterey Bay, California. *Deep Sea Research Part I: Oceanographic Research Papers*, *113*, 22-32. https://doi.org/ 10.1016/j.dsr.2016.04.004

Watanuki, Y., & Thiebot, J. B. (2018). Factors affecting the importance of myctophids in the diet of the world's seabirds. *Marine Biology*, *165*(4), 79. https://doi.org/10.1007/s00227-018-3334-y

747 Wiebe, P. H., Morton, A. W., Bradley, A. M., Backus, R. H., Craddock, J. E., Barber, V., ... &
748 Flierl, G. D. 1. (1985). New development in the MOCNESS, an apparatus for sampling
749 zooplankton and micronekton. *Marine Biology*, *87*(3), 313-323.
750 https://doi.org/10.1007/BF00397811
751

JGR-Oceans

Supporting Information for

The impact of a Southern Ocean cyclonic eddy on mesopelagic micronekton

Alice Della Penna[1,2], Joan Llort[3], Sebastien Moreau[4], Ramkrushnbhai Patel[5,6], Rudy Kloser[7], Peter Gaube[8], Peter Strutton[5], Philip Boyd[5];

1. Institute of Marine Science, University of Auckland, New Zealand
2. School of Biological Sciences, University of Auckland, New Zealand
3. Barcelona Supercomputing Center, Barcelona, Spain
4. Norwegian Polar Institute, Fram Center, Tromsø, Norway
5. Institute for Marine and Antarctic Studies (IMAS), University of Tasmania (UTas), Hobart, Tasmania, Australia
6. Australian Research Council Centre of Excellence for Climate System Science, University of Tasmania, Hobart, Tasmania, Australia
7. CSIRO Oceans and Atmosphere, GPO Box 1538, Hobart, Tasmania, 7001, Australia
8. Applied Physics Laboratory, University of Washington, Seattle, Washington, United States of America

Contents of this file

Tables

	North of the SAF	**South of the SAF**
Daytime	285	188
Night-time	174	128
Total	459	316

Table S1: Duration of sampling in hours for the different subregions extracted from the IMOS dataset

Figures

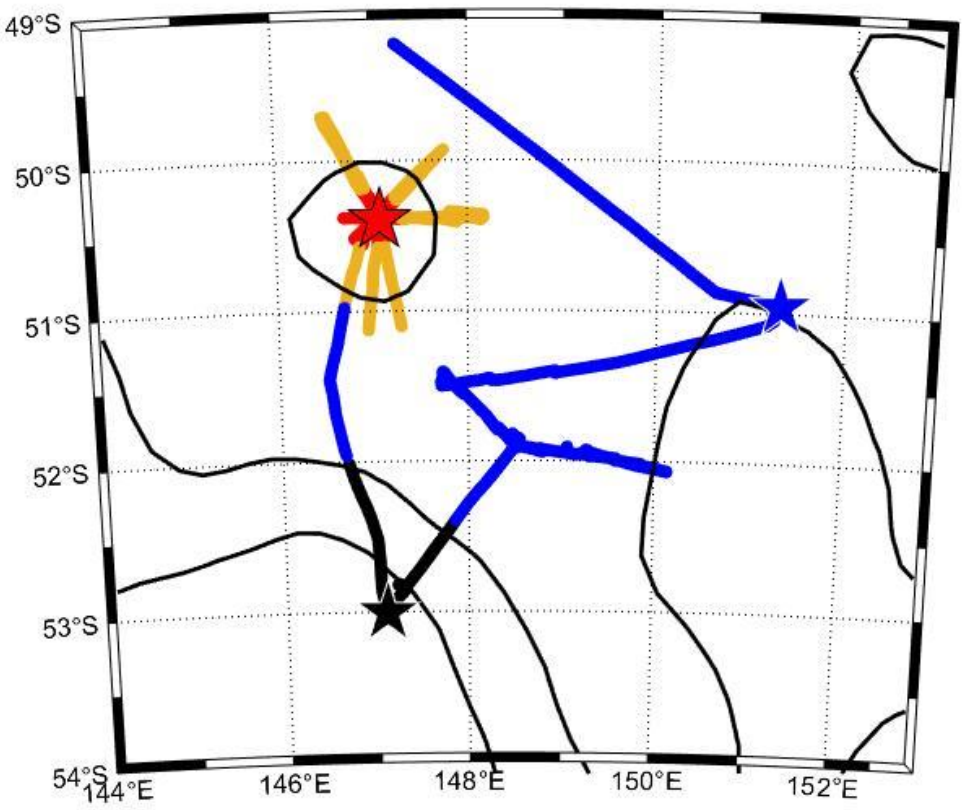

Figure S1: Map representing the sampling of the Sub Antarctic Zone (SAZ, blue), Sub Antarctic Front (SAF, black) and the eddy's core (red) and periphery (ochra). Stars (in red, black and blue) indicate the locations used as examples in Figure 3. Black contours show the -0.4 m and 0.2 m contours of Sea Surface Height corresponding to the northern and southern flank of the SAF during the study period, and the location of the eddy.

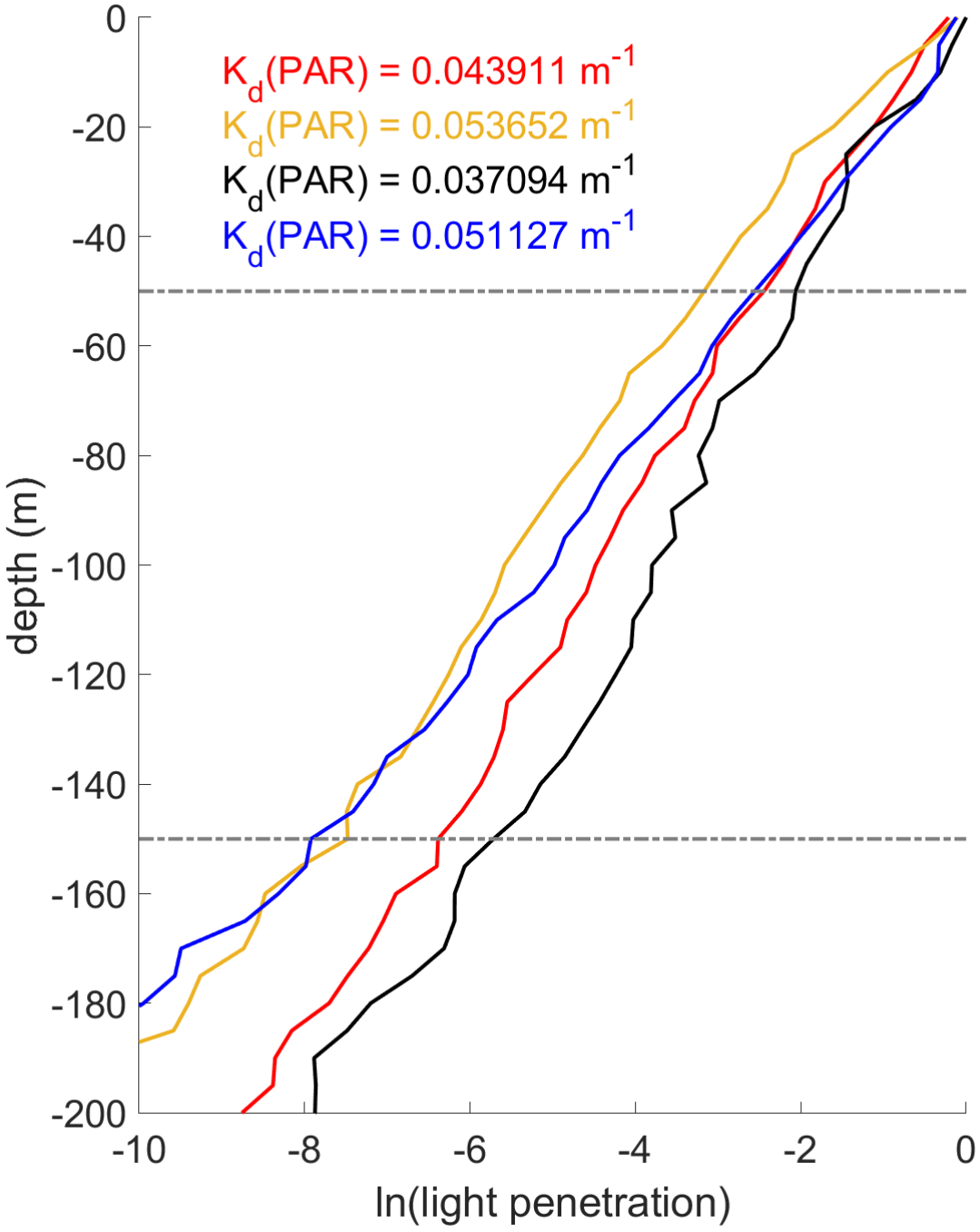

Figure S2 Estimation of the average light attenuation coefficient for the different subregions of this study. Red: eddy core, ochre: eddy periphery, black: PFZ, and blue: SAZ. The grey dashed lines indicate the interval between 50-150 m depths were the irradiance profiles were assumed to be logarithmic and their values used to estimate k_d(PAR).

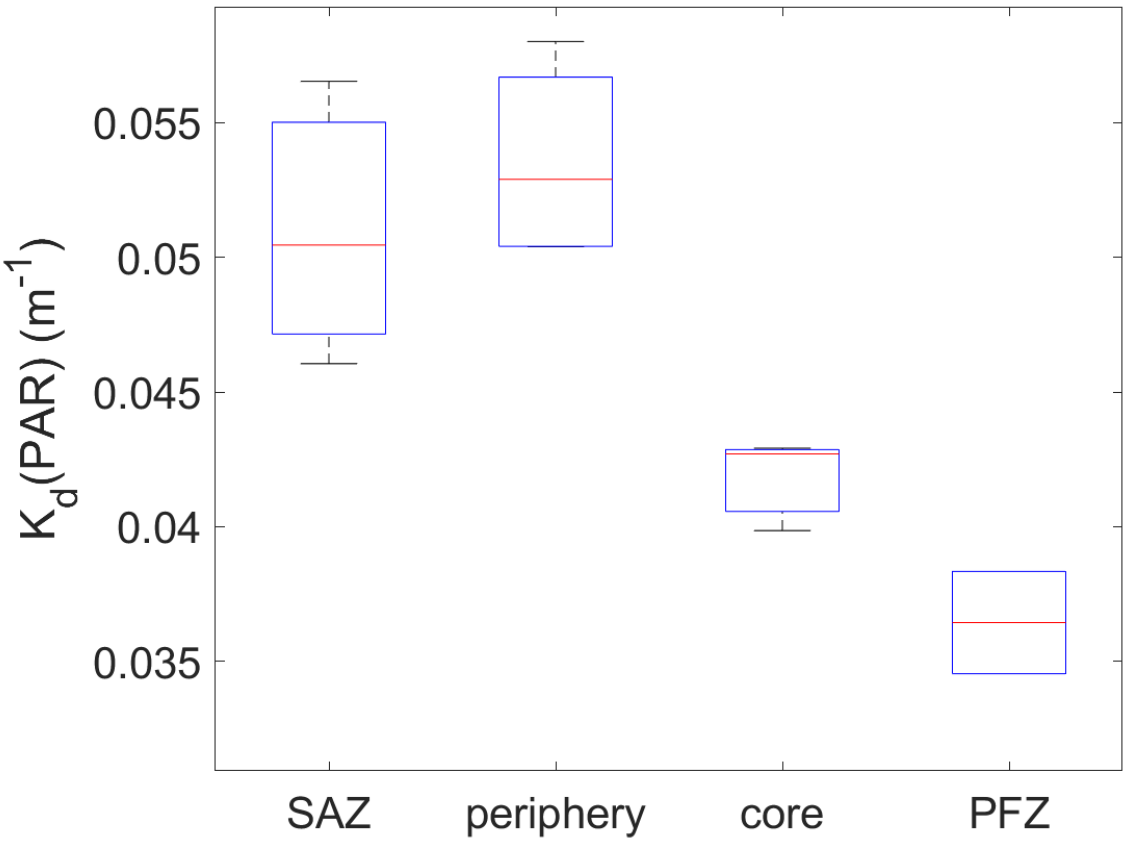

Figure S3 Distribution of K_d(PAR) across the subregions of this study. A Student's t-test confirmed that the differences between the eddy core and the periphery ($p<0.05$) and the SAZ waters ($p<0.05$) are statistically significant, while the differences between PFZ are considerably smaller and might be a result of the limited sample size of our observations ($p=0.07$).

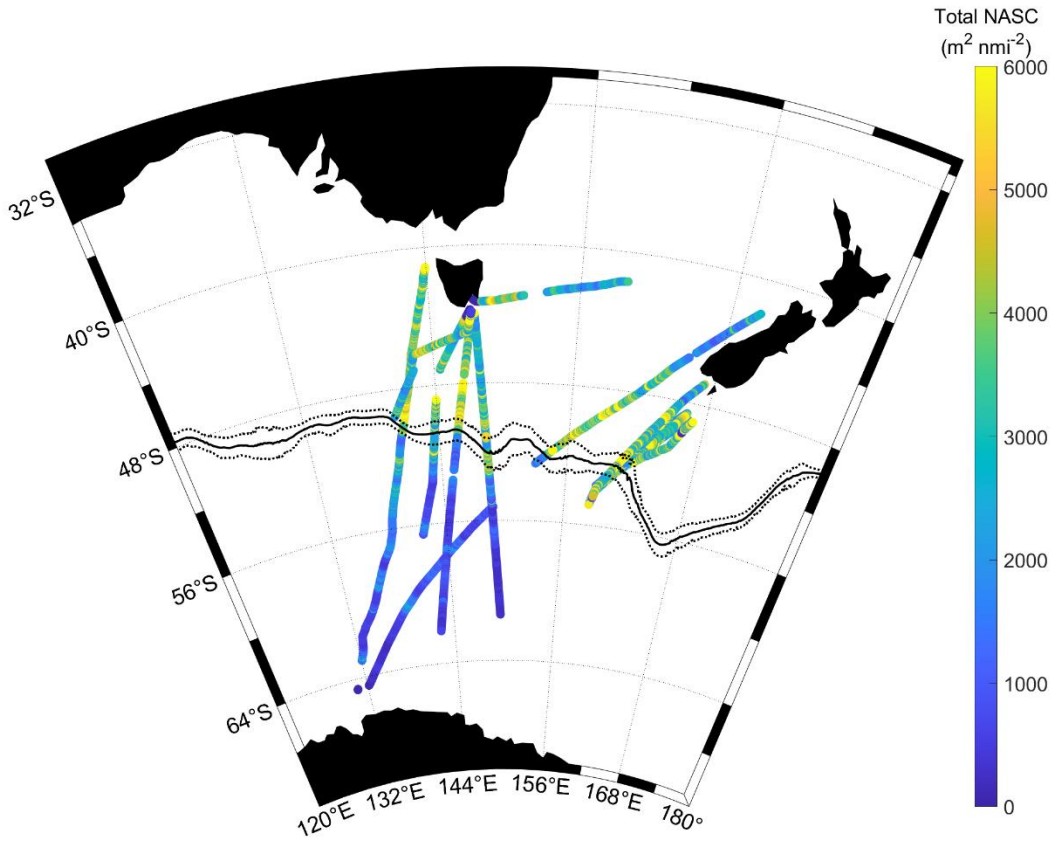

Figure S4 Historical observations of acoustic backscattering at 18 kHz from the IMOS database. The solid black line indicates the average location of the Sub-Antarctic Front, estimated using Sea Surface Height maps. Dashed lines indicate the standard deviation of the latitude of the front.

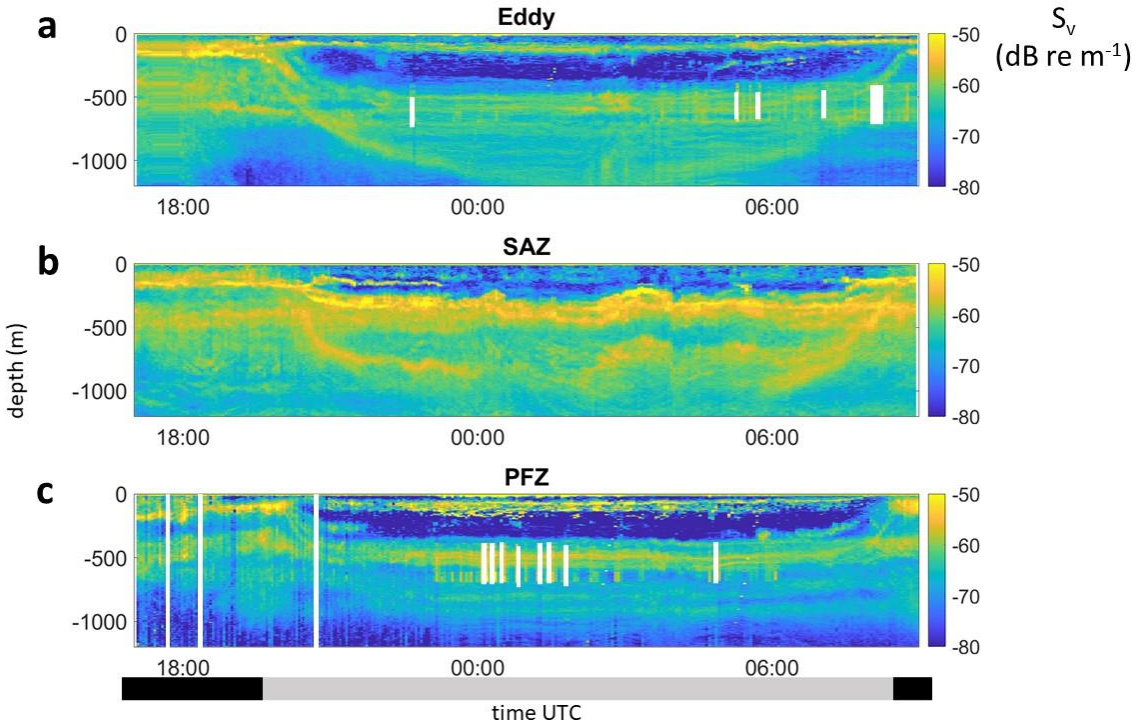

Figure S5: Examples of daytime echograms inside the eddy core (a, referring to 2016/4/4), in the surrounding SAZ waters (c, referring to 2016/4/12) and in the PFZ(d, referring to 2016/4/6) where the eddy was originated.

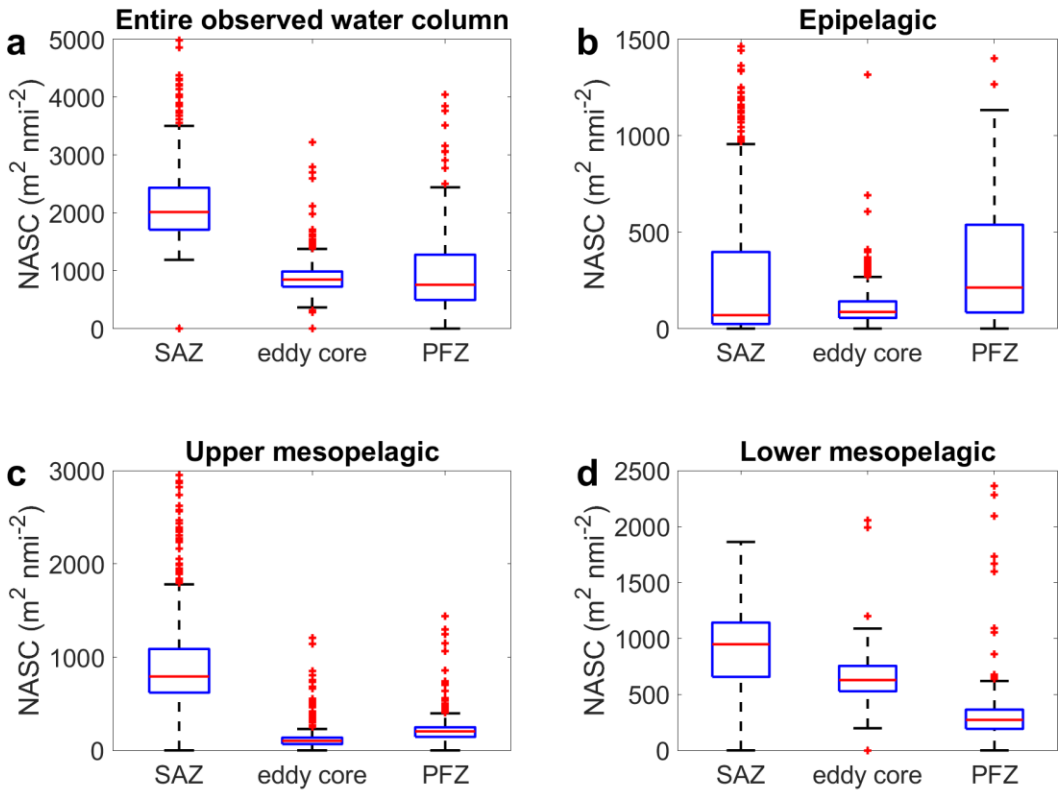

Figure S6 Integrated values of daytime acoustic backscattering in the Sub-Antarctic Zone (SAZ), eddy core, and Polar Front Zone (PFZ). These diagnostics were calculated for the entire observed water column (down to 1200 m, a), for the epipelagic (20-200m, b), the upper mesopelagic (200-600m, c) and lower mesopelagic (600-1200m,d).

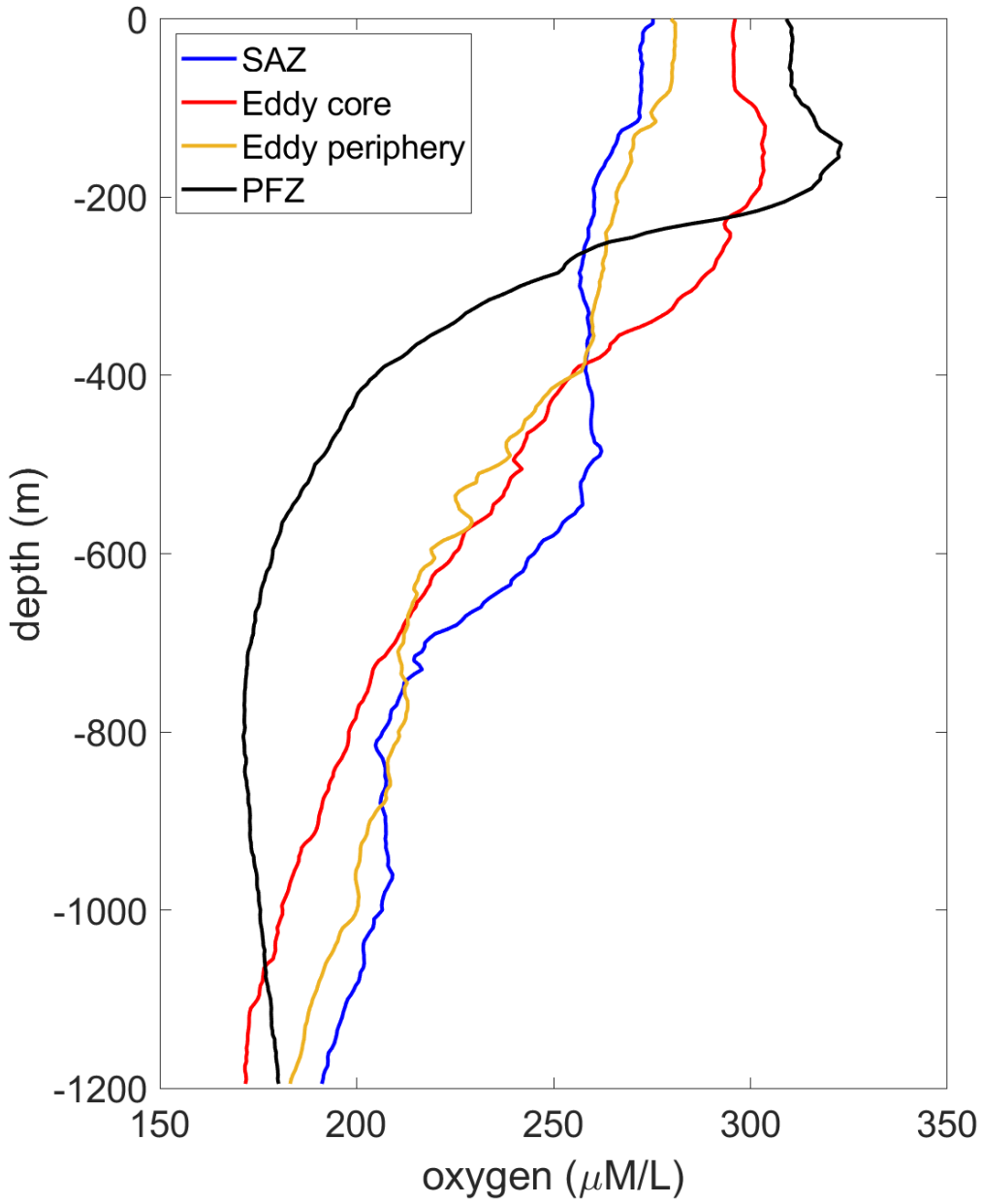

Figure S7 Average profiles of oxygen concentration for the different subregions of this study. Oxygen was measured during the same CTD casts as the ones used to estimate the light attenuation coefficients using a photometric oxygen system (Patel et al., 2020). We observed significant differences in oxygen concentration between the eddy core (red line) and both its origin (PFZ, black line), and SAZ and eddy periphery waters (blue and ochre lines respectively).